

Turning Your Strength against You: Detecting and Mitigating Robust and Universal Adversarial Patch Attack

Zitao Chen, Pritam Dash, Karthik Pattabiraman
University of British Columbia
{zitaoc, pdash, karthikp}@ece.ubc.ca

Abstract—*Adversarial patch attack* against image classification deep neural networks (DNNs), in which the attacker can inject arbitrary distortions within a bounded region of an image, is able to generate adversarial perturbations that are *robust* (i.e., remain adversarial in physical world) and *universal* (i.e., remain adversarial on any input). It is thus important to detect and mitigate such attack to ensure the security of DNNs.

This work proposes *Jujutsu*, a technique to *detect and mitigate* robust and universal adversarial patch attack. *Jujutsu* leverages the universal property of the patch attack for detection. It uses explainable AI technique to identify suspicious features that are *potentially* malicious, and verify their maliciousness by transplanting the suspicious features to new images. An adversarial patch *continues* to exhibit the malicious behavior on the new images and thus can be detected based on prediction consistency. *Jujutsu* leverages the localized nature of the patch attack for mitigation, by randomly masking the suspicious features to “remove” adversarial perturbations. However, the network might fail to classify the images as some of the contents are removed (masked). Therefore, *Jujutsu* uses *image inpainting* for synthesizing alternative contents from the pixels that are masked, which can reconstruct the “clean” image for correct prediction. We evaluate *Jujutsu* on five DNNs on two datasets, and show that *Jujutsu* achieves superior performance and significantly outperforms existing techniques. *Jujutsu* can further defend against various variants of the basic attack, including 1) physical-world attack; 2) attacks that target diverse classes; 3) attacks that use patches in different shapes and 4) adaptive attacks.

I. INTRODUCTION

Adversarial attacks against deep neural networks (DNNs) have become a topic of great interest since the seminal work of Szegedy et al. [1]. Subsequently, many techniques have been proposed to generate adversarial samples, i.e., inputs with adversarial perturbations to trigger malicious behavior such as image misclassification. Adversarial perturbations that cause misclassification when added to arbitrary inputs are known as *universal attacks* [2], [3], [4], [5], [6], [7], [8].

Adversarial samples can also be synthesized to be *robust* (i.e., physically realizable) in the physical world [7], [9], [10], [11], e.g., a malicious stop sign to trigger targeted misclassification [9], [11]. This has led to *adversarial patch attacks* [7], which create *robust and universal* adversarial samples (also referred to as *patch attack*). These attacks add arbitrary changes to the input images within a region of bounded size, to cause targeted misclassification in common DNNs. They are an important threat as they can entail dire

consequences for real-world systems such as autonomous vehicles and facial recognition. Further, their universal nature drastically lowers the barrier to launch the attack: a universal adversarial patch can be widely distributed to fool arbitrary DNN systems with little to no effort from the attacker.

A number of defenses have been proposed to detect [12], [13], [14], [15] or mitigate [16], [17], [18], [19] adversarial patch attacks. We briefly discuss them below and summarize their limitations (a detailed review is in Section V).

Detection: Chou et al. [12] detect patch attack by transplanting the salient features of an image and patterns like Gaussian noise pattern to a corpus of clean images, after which statistical analysis is conducted to detect the attack. Ma et al. [13] propose to detect patch-like adversarial samples based on invariant checking. Gao et al. [14] detect patch-like trojaned adversarial samples by superimposing the target image with new images and using the prediction entropy for detection.

Mitigation: Naseer et al. [16] propose local gradient smoothing (LGS) to neutralize the effect of adversarial patch pixels. Hayes et al. [19] mitigate patch attack by selectively masking the pixels that have large influence to the output based on pre-defined thresholds. Adversarial training has also been adapted to defend against patch attack [17], [18].

Unfortunately, existing techniques suffer from the following limitations:

- 1) Do not provide attack mitigation [12], [13], [14], [15], which is important for critical systems such as autonomous driving that require adequate attack response.
- 2) Poor characterization of adversarial patch such as not being able to reliably locate the adversarial patch in the image, hence causing low detection performance [12], [14];
- 3) Poor distinction between adversarial and benign pixels, thus yielding high false positive rate (FPR) [13], [16], [17], [18], [15].
- 4) Insufficient mitigation by simply masking the adversarial pixels [16], [19]. The DNNs can still make wrong prediction due to the loss of semantic contents incurred by masking.
- 5) The robust accuracy degrades when confronting attacks that target diverse classes [17], [18].

To overcome these limitations, we propose *Jujutsu*¹ for both detecting *and* mitigating adversarial patch attacks (addressing limitation 1). *Jujutsu* detects adversarial patches by leveraging the universal property that is *unique* to the adversarial patch, which enables accurate detection of adversarial patches and low FPR (addressing limitation 2 and 3). We propose to use *image inpainting*, which effectively allows the DNNs to make correct prediction on adversarial samples (addressing limitation 4). Our detection and mitigation makes use of prediction consistency, which is scalable to attacks targeting diverse classes (addressing limitation 5). We provide a quantitative comparison with existing techniques in Section IV-D and show that *Jujutsu* achieves superior performance.

Detecting adversarial patch attack. Our idea is to exploit the universal nature of the patch attack, which causes the adversarial patch to yield a disproportionately large influence on the final prediction. To do so, we use explainable AI techniques [20], [21], [22] to identify the salient features that are highly influential on the final prediction. However, salient features can also contain benign features (e.g., foreground objects), and hence explainable AI methods are by themselves *insufficient* to distinguish malicious features from benign ones.

Therefore, we need a technique to distinguish adversarial features from the benign ones. To do so, we exploit the fact that the patch will cause misclassification on any image as it is universal. Specifically, we transplant the salient features from the original input to the *least-salient* regions of the new hold-out inputs, and compare the prediction label on the original and new image. An adversarial patch is detected if (and only if) the predictions on both images result in the *same* label. The reason is, if the salient features of the original input contain adversarial patch, transplanting these salient features to a new input will result in targeted misclassification. This is a *unique* property of the adversarial patch.

Mitigating adversarial patch attacks. Adversarial patch attack requires the adversarial perturbations to be confined within a contiguous localized region. Therefore, upon detecting the adversarial sample, we could randomly mask the salient features, which would remove the adversarial perturbations. However, this would result in the loss of semantic contents, and the network might not be able to derive the correct prediction label. Therefore, we use *image inpainting* (i.e., image completion), a technique to synthesize the missing contents in the images to restore the missing semantic contents of the pixels that are masked, and attempt to reconstruct the “clean” image for correct prediction.]

Contributions. The contributions of our work are:

- Propose a method to identify image features that are potentially malicious, and determine whether they are truly malicious using feature transfer and prediction consistency.
- Design a parametric masking technique to remove adversarial pixels, thereby converting the adversarial patch to a non-

adversarial one. The parametric property allows balancing the detection of adversarial samples and FPRs.

- Introduce the use of image inpainting to synthesize the missing contents in the pixels that are masked. This allows the DNNs to generate correct predictions on the adversarial samples, and reduce FPRs.
- Evaluate *Jujutsu* on five DNNs on two datasets and show that *Jujutsu* achieves superior performance and significantly outperforms existing defenses: LGS [16], STRIP [14], SentiNet [12], and adversarial training.
- Demonstrate the effectiveness of *Jujutsu* against different variants of the basic attack: 1) physical-world attack, 2) attacks that target diverse classes, 3) attacks that use patches of different shapes and 4) adaptive attacks.

II. BACKGROUND

A. Attack Formulation

Denotations: We express a DNN as $F_\theta : X \rightarrow Y$, where $X \in \mathbb{R}^n$ and $Y \in \mathbb{R}^m$ denotes the input and output space, and F is parameterized by weights θ (θ is omitted for simplicity in this work). Pixel intensity is rescaled from $[0, 255]$ to $[0, 1]$. \bar{y}_i is the ground truth label and $\hat{y} = \operatorname{argmax}_{F_\theta}(x)$ the prediction label with the highest probability.

This work primarily considers the patch attack by Brown et al. [7]. Note that there is another variant of patch attack called LaVAN attack [23], which is similar in spirit to that of Brown et al. with a slightly different objective function. However, LaVAN attack is *not* robust to physical transformations and *not* universal. The procedure to make LaVAN attack robust and universal is similar to that by Brown et al, thus we focus on the attack formulation by Brown et al.

We call an input $x' \in X$ an adversarial sample if

$$x' \in X \wedge \operatorname{argmax} F(x') = y^{adv} \wedge \operatorname{argmax} F(x) = \bar{y}, \quad (1)$$

where y^{adv} is the target class as we consider targeted misclassification, x' is the adversarial sample generated from the original input x , which is correctly classified by the network. The patch attack is created by completely replacing a part of the image with the image patch, denoted as $\delta \in \mathbb{R}^n$. Thus the generation of adversarial sample x' can be represented as:

$$x' = (1 - m) \odot x + m \odot \delta, \quad (2)$$

where $m \in \{0, 1\}^n$ is a mask used to replace the original pixels with the adversarial patch ($\forall m_i \in m, m_i = 1$ is where the patch will be placed), \odot is element-wise multiplication, δ is the adversarial image patch.

To make patch δ be universal (i.e., input-agnostic), the patch is trained over a variety of images. For each input $x \in X$, patch δ can be applied in any random location L .

To make patch δ robust (i.e., physically realizable), Brown et al. propose to use a variant of Expectation over Transformation (EOT) framework [10]. EOT is used for a distribution of environmental transforms T that transform x to different physical environments (e.g., translation, rotation, lightness changes), under which the adversarial samples aim to remain robust.

¹Jujutsu is a martial art whose philosophy is to manipulate the opponent’s force against him- or herself rather than confronting them with one’s own force. Our technique has a similar philosophy, and hence the name.

Based on the above, the objective function of the patch attack can be formulated as:

$$\delta = \underset{\delta}{\operatorname{argmax}} \mathbb{E}_{x \sim X, t \sim T, l \sim L} [\log \Pr(y = y^{adv} | x')], \quad (3)$$

where X is a set of training images to train the adversarial patch, T is a distribution of transformations over the patch, and L is a distribution over locations in the images. By applying EOT over a batch of images, the optimization in Equation 3 allows the patch to work regardless of the background.

B. Threat Model

This work assumes a white-box attacker, who has full knowledge of the victim DNN such as its structure, parameters and training procedure. We assume however that the attacker has no knowledge of the exact inputs to the DNN, but instead has access to a surrogate dataset, which follows the same distribution as the legitimate inputs (but has no intersection with them). This is similar to the assumptions in universal attack studies, and it is shown that the knowledge of the input distribution often suffices for the attacker to generate universal adversarial perturbations [2], [3], [4], [5], [6], [24].

We assume the defender has exclusive access to a hold-out dataset coming from the same data distribution. Such a hold-out dataset can be created by randomly sampling a series of images from the data distribution (e.g., drawing 1000 random images from over 1 million images in ImageNet dataset).

The attacker is allowed to replace a contiguous region of an image with the adversarial patch. As in most prior works, we primarily consider square patch [16], [25], [26], [27], [28]. Further, *Jujutsu* can generalize to other shapes such as circular and rectangular patches, and we provide experimental results in Section IV-G. The attacker’s goal is to generate a robust and universal adversarial patch that can trigger targeted misclassification in the DNNs.

III. METHODOLOGY

A. Design Overview

We first explain the main observations of the patch attack that underpin the design of *Jujutsu*.

- 1) The universal and localized feature of adversarial patch requires the adversarial pixels to have a *disproportionately large* influence on the output, in order to trigger targeted misclassification universally. This is because the perturbations (1) are confined to a small number of pixels in the image, and (2) need to exhibit the malicious behavior to cause targeted misclassification on arbitrary input.
- 2) The robust nature of patch attack requires the perturbations to be localized (visible) so as to survive under real world environments (small and imperceptible perturbations are vulnerable to physical transformations [29]). Hence, physical attack can be modeled as localized adversarial patches.

Fig. 1 illustrates the procedure for attack detection (based on Observation 1) and Fig. 2 for attack mitigation (based on Observation 2). They are as follows.

Detecting adversarial patch. The first step is to identify suspicious features that potentially contain adversarial patch,

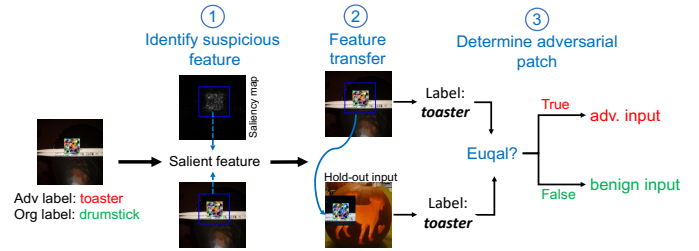


Fig. 1: Detection of adversarial patch. Step 1: Identify suspicious features that might contain adversarial patch. Step 2: Transfer the suspicious features to the new hold-out input. Step 3: Determine the adversarial patch based on prediction consistency.

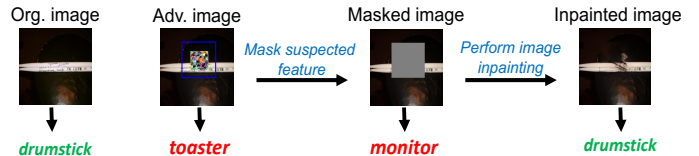


Fig. 2: Mitigation of adversarial patch: (randomly) mask the suspicious features in the blue box, and perform image inpainting to synthesize the contents in the mask.

by using explainable AI techniques [20], [21], [22] to compute the saliency map, which models the contribution of different input features towards the final prediction. From the saliency map, we can extract the region of inputs that are particularly influential on the final prediction, e.g., the area in the blue box in Fig. 1 (henceforth, called *saliient features*). These features are considered suspicious as they have a large influence on the output, similar to the adversarial patch’s behavior.

However, the suspicious features *do not* necessarily contain adversarial pixels, because benign features in the foreground objects could also have a large influence on the output. Therefore, we extract the suspicious features from the original input, and transplant them to the hold-out input set (Step 2 in Fig. 1) Step 3 compares the prediction on the original input and the hold-out input implanted with the suspicious features. If both predictions lead to the *same* prediction label, the suspicious features is marked as adversarial.

Mitigating adversarial patch. The goal of mitigation is to remove the attack’s effects, and allow the DNN to predict the correct label from the adversarial samples. A straightforward solution is to mask out the suspicious features so that the adversarial patch will not contribute to the final prediction. Unfortunately, masking alone does not work in many situations. For instance, in Fig. 2, masking the suspected feature can undo the targeted classification, and the DNN no longer predicts the adversarial sample as a “toaster” (the target label determined by the attacker), thus defying the attack. However, the DNN predicts the image with the mask as a “monitor”, which is not the correct label for the image. This shows that merely masking the suspected feature also removes the semantic contents in the image, and hence the DNN is *not* able to predict the correct label from the masked images.

To remove the effects of the attack without removing the semantic contents, we use *image inpainting* (i.e., image completion) [30], [31], [32], a technique for synthesizing

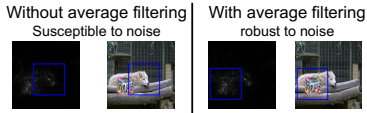


Fig. 3: Visual comparison of extracting suspicious features from the saliency map with and without average filtering. The former is susceptible to noise while the latter is not. We use average filtering.

alternative contents from the missing regions in images. In our context, image inpainting can be used to reconstruct the missing semantic contents from the pixels that are masked, resulting in a “clean” image that is free from corruptions for the DNN to make correct prediction. As shown in Fig. 2, after performing inpainting on the masked image, the DNN is able to correctly predict the image as a “drumstick”. We use the prediction label of the inpainted image as the final output.

B. Detecting the Adversarial Patch

Step 1. We first compute a saliency map that provides explanation by modeling the contributions of different pixels on the final decision. One common approach is to compute the gradients of the output with respect to the input pixels. Mathematically, the saliency map $M_j(x)$ can be expressed as: $M_j(x) = \partial F(x)_j / \partial x$, where j indicates the class label. $M_j(x)$ represents how much difference a tiny change in each pixel of x would contribute to the output $F(x)_j$. Thus $M_j(x)$ can be used to highlight the key regions in predicting $F(x)_j$.

We use SmoothGrad [20], which can help visually sharpen the gradient-based saliency map and smooth out the noisy gradients (that arise due to the local variations in partial derivatives [20]). Other methods such as Grad-cam [22], Integrated Gradient [33] can also be used. Given the noisy (fluctuating) gradients, SmoothGrad computes a local average of the gradient values, by taking random samples in the neighborhood of an input x , and averaging the resulting saliency maps. This operation can be expressed mathematically as:

$$\hat{M}_j(x) = \frac{1}{n} \sum_1^n M_j(x + \mathcal{N}(0, \sigma^2)), \quad (4)$$

where n is the number of samples, and $\mathcal{N}(0, \sigma^2)$ represents the Gaussian noise with standard deviation σ .

To extract the suspicious features (i.e., adversarial patch) from the saliency map, one approach is to choose the point that has the maximum value within the saliency map, and draw a detection box around it. However, this approach is susceptible to noise, e.g., a single large-value pixel outside the adversarial patch could result in a mis-identification and thus the detection box would fail to locate the patch. Therefore, we perform an *average filtering* over the saliency map to make it more robust to noise, thereby allowing us to accurately locate the region of adversarial patch. A visual comparison of the approaches in identifying the suspicious features is in Fig. 3.

Step 2. We next transfer the suspicious features from the original input to the hold-out input in order to determine whether they are truly malicious. One way is to randomly transplant the suspicious features to the new hold-out input and compare the prediction. However, randomly transplanting the

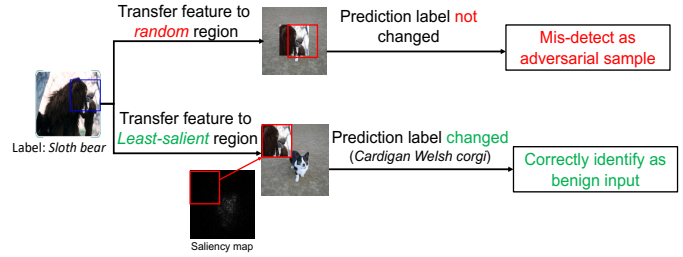


Fig. 4: Different strategies to transfer features. In the upper side, the suspicious features are transplanted to a *random* location of the hold-out input which leads to a mis-detection, while those in the lower side are transferred to the *least-salient* region of the hold-out input, and thus the original input is correctly identified as benign.

suspicious features may result in overlap with the foreground object in the hold-out input. Should this happen, the prediction labels on the original and hold-out input may become the same, which would lead to a mis-detection of benign input, i.e., a FP. Fig. 4 shows an example, where randomly transplanting the benign features to a new hold-out input leads to the same prediction label (both images result in a label of “Sloth bear”), thus resulting in a FP.

To avoid FP, we transplant the suspicious features to the *least-salient* regions of the hold-out input, which could minimize the chances that the suspicious features override the images’ natural features. The least-salient regions are those regions that have *low* influence on the output according to the saliency map. Only those suspicious features containing the adversarial patch at the least-salient regions will also lead to the same prediction label (due to the patch’s universal nature). Fig. 4 shows how this method works.

Step 3. The final step to determine the adversarial sample is to compare the prediction labels on the original and hold-out images implanted with suspicious features. The original image is deemed to be adversarial if and only if both images yield the same prediction label. This is because only the suspicious features that contain the adversarial patch will cause (the same) misclassification on the hold-out input. We are also able to identify suspicious features that come from the benign features, by checking whether the prediction labels on the original and hold-out images implanted with suspicious features are *different*. We consider an image to be benign if the prediction labels are different.

C. Mitigating the Adversarial Patch

The mitigation of patch attack has two steps: (1) converting the adversarial patch to a non-adversarial one, i.e., it fails to cause targeted misclassification. (2) Correct inference of the corrupted input, despite the patch. Note that simply making the adversarial patch non-adversarial does not mean that the DNN is able to predict correctly. For instance, in Fig. 2, masking all the suspicious features disrupts the targeted misclassification, but the DNN fails to infer the correct label.

1) *From Adversarial to Non-adversarial:* For the first problem, one can mask the *entire* set of suspicious features, which would remove all the adversarial pixels, and allow the DNN to perform inference based on the rest of the untainted pixels.

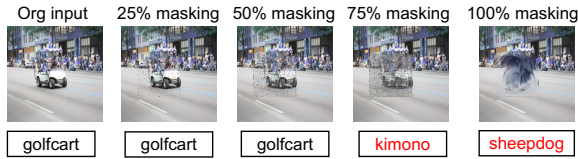


Fig. 5: How masking different amount of pixels would affect the FP (mis-detection) on benign inputs. Assume the original input is mis-detected as an adversarial one. If the labels on the original and the inpainted input (column 2-3) are the same, the mis-detection can be rectified. Column 4-5 would result in mis-detection.

However, this would have adverse effects and cause incorrect prediction of the output. We find that it is often *unnecessary* to mask all the pixels. Instead, randomly masking a portion of the adversarial pixel suffices to convert the adversarial patch to a non-adversarial one. For example, masking 75% of the suspected features in our experiments is able to convert over 99.9% of the adversarial patches to non-adversarial ones. Therefore, we introduce a *parametric masking* technique, which allows the defender to control the amount of pixels to mask in the suspected adversarial patch.

We can determine a mis-detection on the benign input (i.e., FP) if the predictions on both the original and inpainted images result in the same label (to be discussed in Section III-C3). The fewer pixels to be masked, the better is the quality of the resulting inpainted image, because more semantic information is preserved in the image.

Fig. 5 shows an example of the inpainted images under different masking percentages. Assume the original input is mis-detected as adversarial - we can eliminate this mis-detection if the original and inpainted image have the same label. In this example, if 25% or 50% of the pixels are masked, *Jujutsu* is able to rectify the mis-detection. However, if 75% or 100% of the suspicious features are masked, the DNN is unable to generate the correct prediction on the inpainted image, thus resulting in a FP. This explains why masking the entire suspicious features could be undesirable.

2) *Correct Prediction from the Corrupted Input*: When performing pixel masking on the image to remove the attack effects, it is unavoidable for some of the semantic contents to be lost. However, we find that this loss can be alleviated by *synthesizing the alternative contents* in the pixels that are replaced by the attacker. To this end, we use image inpainting, a technique typically used for filling the missing pixels of an image in computer vision [30], [31], [32], [34]. In our work, image inpainting is used to reconstruct the contents replaced by the adversarial patch, and to increase the probability that the DNN predicts the correct label. *To the best of our knowledge, our work is the first to use image inpainting for mitigating adversarial patch attack.*

There are many image inpainting techniques proposed in the literature. We use, Pluralistic Image Completion DNN (PICnet) [32], a recent image inpainting technique, which can generate multiple and diverse plausible contents from the mask. Although we choose PICnet in this work, other inpainting techniques [30], [31], [34] may also be considered

as our goal is to synthesize semantically meaningful contents in the mask, which is a common task for inpainting techniques.

Formally, let x be the original image, x_m the image with a region of pixels being masked, and x_c the original pixels that are masked. PICnet synthesizes diverse contents from the mask by sampling a conditional distribution $p(x_c|x_m)$. In the training phase, PICnet uses a *reconstructive* pipeline, in which the missing regions x_c are encoded into the latent space representation in a continuous distribution that can be sampled to rebuild the diverse and plausible x_c . The reconstructive pipeline leverages x_c and x_m to reconstruct x in a supervised manner (x_c is the ground truth). In testing phase, PICnet uses a *generative* pipeline to infer the conditional distribution of $p(x_c|x_m)$, which is sampled to generate x_c . The parameters in the reconstructive pipeline are shared with the generative pipeline so that it can reconstruct x from x_m during testing.

The resulting inpainted images are meant to be free from adversarial perturbations, and thus we use the labels on the inpainted images as the final output for mitigation.

3) *Reducing FPRs*: Masking and inpainting can also be used to reduce the FPR due to mis-detections. Specifically, we signal a mis-detection when the prediction label on the original input (that *Jujutsu* originally detected as adversarial) and the inpainted input are *identical*. The intuition is that a benign input does not contain an adversarial patch, and hence predictions based on the original and the inpainted images should both result in the same prediction label. Our example in Fig. 5 illustrates this.

The above process to reduce FPR might also inadvertently regard some adversarial samples as the benign ones. For example, if the masking percentage is low, the adversarial patch will continue to cause misclassification on the inpainted images, based on which *Jujutsu* would incorrectly flag the adversarial patch as a benign patch. We study how different masking percentages would affect the detection in our evaluation.

D. Overall Algorithm

Algorithm 1 shows the overall algorithm of *Jujutsu*. The inputs are the images to be classified and parameters for *Jujutsu*. For each x_i , the output includes the prediction label y_{x_i} and a flag $isAdv_{x_i}$ on whether x_i is adversarial. Lines 4-8 extract the salient features from x_i . Lines 10-15 identify the least-salient regions in the hold-out input x^* , which will be replaced by the salient features from x_i . Lines 16-25 perform feature transfer and compare the prediction labels on the original and new implanted image. Lines 29-39 perform attack mitigation by accepting the label from the inpainted image, and checking for mis-detections (thereby reducing FPs).

IV. EVALUATION

In this section, we first describe the experimental setup in Section IV-A. We then answer the following research questions (RQs) in the following sections.

RQ1: What's the detection performance of *Jujutsu*?

RQ2: What's the mitigation performance of *Jujutsu*?

RQ3: How does *Jujutsu* compare with existing techniques?

Algorithm 1 Detect and mitigate patch attack

Input: X_{test} : Test images; X_{hold} : Hold-out images; F : DNN model;
 l : Length of detection box; p : Percentage of pixels to mask
Output: Y_{test} : Prediction on X_{test} ; $isAdv_{X_{test}}$: whether X_{test} is adversarial

```
1: function DETECTION( $X_{test}, X_{hold}, F, l$ )
2:   for each  $(x_i, y_{x_i}, isAdv_{x_i}) \in (X_{test}, Y_{test}, isAdv_{X_{test}})$  do
3:      $y_j = \operatorname{argmax} F(x_i)$ 
4:     // Extract the salient features  $B_{x_i}$  from  $x_i$ 
5:      $M_j(x_i) = \operatorname{SmoothGrad}(x_i, y_j)$  // Saliency map for  $(x_i, y_j)$ 
6:      $M_j(x_i) = \operatorname{AverageFilter}(M_j(x_i))$  // Average filtering over saliency map
7:      $(x_{max}, y_{max}) = \operatorname{MaxLoc}(M_j(x_i))$  // point with maximal value
8:     Draw a box  $B_{x_i}$  around  $(x_{max}, y_{max})$  with length  $l$  // suspicious features
9:     // Identify the least-salient features  $B_{x^*}$  from  $x^*$ 
10:    Randomly select  $x^* \in X_{hold}$ 
11:     $y_k^* = \operatorname{argmax} F(x^*)$ 
12:     $M_k(x^*) = \operatorname{SmoothGrad}(x^*, y_k^*)$  // Saliency map for  $(x^*, y_k^*)$ 
13:     $M_k(x^*) = \operatorname{AverageFilter}(M_k(x^*))$  // Average filtering over saliency map
14:     $(x_{min}^*, y_{min}^*) = \operatorname{MinLoc}(M_k(x^*))$  // point with minimal value
15:    Draw a box  $B_{x^*}$  around  $(x_{min}^*, y_{min}^*)$  with length  $l$ 
16:    // Feature transfer and prediction comparison
17:     $x^{**} = x^*.replace(B_{x^*}, B_{x_i})$ 
18:     $y_k^{**} = \operatorname{argmax} F(x^{**})$ 
19:    if  $y_k^{**} == y_j$  then
20:       $y_{x_i}, isAdv_{x_i} = \operatorname{MITIGATION}(x_i, B_{x_i}, F, p)$  //  $x_i$  is adversarial
21:    else
22:       $y_{x_i} = y_j$  //  $y_j$  is the prediction label from line 3
23:       $isAdv_{x_i} = \text{False}$  //  $x_i$  is benign
24:    end if
25:  end for
26:  return  $Y_{test}, isAdv_{X_{test}}$ 
27: end function
28:
29: function MITIGATION( $x, B_x, F, p$ )
30:    $y_{org} = \operatorname{argmax} F(x)$ 
31:    $x_{mask} = \text{Randomly mask } p\% \text{ of pixels within } B_x \text{ in } x$ 
32:    $x_{inpaint} = \operatorname{PICNet}(x_{mask})$  // Perform inpainting
33:    $y_{new} = \operatorname{argmax} F(x_{inpaint})$ 
34:   if  $y_{org} \neq y_{new}$  then
35:     return  $y_{new}, \text{True}$  // Attack mitigation
36:   else
37:     return  $y_{org}, \text{False}$  // Reduce false positive
38:   end if
39: end function
```

RQ4: Can *Jujutsu* detect and mitigate physical-world attack?

RQ5: Can *Jujutsu* detect and mitigate attacks that target different classes?

RQ6: Can *Jujutsu* detect and mitigate attacks that use patches in different shapes?

RQ7: Is *Jujutsu* able to make the DNNs more robust even under adaptive attacks?

A. Experimental Setup

1) *Hardware and Software Framework:* Our experiments used the following machines: 1) an Ubuntu Linux 18.04.2 system with 8 RTX 2080Ti GPUs, 24 CPUs and 256 GB memory; 2) a Fedora Linux 20 system with 2 GTX TITAN GPUs, 16 CPUs and 256 GB memory. We use PyTorch 1.0.0 and Torchvision 0.2.1 [35] as the ML framework. We use two datasets: the 1000-class ImageNet dataset [36] and the 10-class ImageNette dataset [37]. We consider five commonly used DNN models: ResNet-50 [38], ResNet-152 [38], VGG16 [39], DenseNet-121 [40] and SqueezeNet [41]. All ImageNet models use the pre-trained weights from the Torchvision library, and we train the ImageNette models for evaluation (training details are available in Appendix C).

2) *Attack Setup:* We use the code on Github [42] to generate the adversarial patch by [7]. We fix the target label

as “toaster” for ImageNet (which is in line with [7]) and “French horn” for ImageNette². For the evaluation on digital images, we consider the digital representation of the patch attack, while omitting the robustness to viewpoint changes and printability issues. We do however consider the actual implementation (i.e., print-out) of the patch attack when evaluating the physical-world patch attack (Section IV-E).

We use 2000 random images from the validation set for training the patches, and 2000 separate images as the test set for evaluating the resulting patches. We only consider those images that can be correctly classified by the networks. The generated adversarial patch is inserted at a random location within each image. We set the probability threshold to 0.9, i.e., the adversarial image is classified as the target label with a confidence score of at least 90%. We set the learning rate as 1.0 and the maximal step per image as 1000.

We consider adversarial patches that occupy 4%, 5% and 6% of the image. We use the term $x\%$ patch to refer to a patch that occupies $x\%$ of the pixels of the image it resides in. We do not consider patches of smaller size because we find that they are unable to universally cause misclassification in the network, e.g., a 2% patch in ResNet-50 on ImageNet yields an attack success rate of just 6.22% in 30 epochs. We do not consider patches of larger size because a 6% patch is able to yield very high attack success rates on the DNNs (96.88% on average). Increasing the patch size will further increase the attack success rate, and *Jujutsu* will still be able to detect these larger patches based on their universal property. We train each patch for 30 epochs and use the one with the highest attack success rate on the test set.

3) *Technique Setup:* We use an open-source program [43] to generate the saliency map. For Equation 4, we follow [20] to set $\sigma = 0.1$ and $n = 50$, i.e., applying 10% of noise to 50 noisy variants of each input. We use `cv2.blur` from the Python `cv2` library with a filter size of 51 to pre-process the saliency map to make it robust to noise. We then identify the point with the highest value in the saliency map as the center of the detection box. The length of the detection box is set to 102, which is around 20% of the pixels in the images. We sample a total of 1000 random images as the hold-out dataset.

For each image, we empirically choose 2 random images from the the hold-out dataset for feature transfer as we find that this setup balances the detection success recall and FPR. We show in Appendix B *Jujutsu*’s performance when we use different number of random images from the hold-out dataset.

For image inpainting, we use the implementation of PICNet [44]. The original implementation does not support pixel-wise random masking, and we added this feature.

Our code is publicly available at <https://github.com/DependableSystemsLab/Jujutsu>.

²While we choose one target class for each dataset, *Jujutsu* is able to detect and mitigate attacks targeting diverse classes as it does not rely on the details of the prediction label. We provide experiment results in Section IV-F.

TABLE I: *Jujutsu*'s detection performance in terms of detection success recall on adversarial samples and detection FPR on benign inputs.

Model	Patch Size	ImageNet				ImageNette			
		Clean Accuracy	Attack Success Rate	Detection Success Recall	Detection FPR ¹	Clean Accuracy	Attack Success Rate	Detection Success Recall	Detection FPR ¹
ResNet-50	6%		97.09%	99.18%	8.72%		99.20%	99.45%	1.20%
	5%	75.60%	93.65%	97.11%	8.67%	75.00%	98.60%	97.95%	3.65%
	4%		76.72%	86.72%	5.69%		95.66%	97.55%	2.70%
DenseNet-121	6%		99.12%	98.77%	9.05%		99.26%	98.20%	3.75%
	5%	73.65%	98.10%	99.17%	7.69%	81.80%	99.16%	99.55%	2.70%
	4%		95.45%	97.37%	9.32%		98.25%	98.55%	2.70%
SqueezeNet	6%		97.92%	97.79%	2.68%		98.37%	99.10%	0.85%
	5%	55.40%	94.67%	96.09%	2.10%	62.00%	95.64%	98.80%	0.85%
	4%		82.75%	84.61%	1.64%		91.55%	98.55%	0.85%
VGG16	6%		94.21%	92.34%	7.23%		95.88%	99.50%	4.15%
	5%	73.50%	92.85%	93.26%	8.14%	76.50%	94.17%	95.85%	4.15%
	4%		77.94%	74.85%	5.85%		85.66%	98.10%	4.15%
ResNet-152	6%		97.56%	99.34%	7.23%		99.55%	85.10%	4.15%
	5%	78.00%	97.31%	98.55%	8.14%	76.00%	98.95%	88.84%	4.15%
	4%		88.84%	94.22%	5.85%		95.76%	77.59%	4.60%
Average	N/A	71.23%	92.14%	93.96%	7.44%	74.26%	96.38%	95.51%	2.98%

¹ Note that the FPR can be further reduced by the combination of detection of mitigation, to be evaluated in Table II.

B. RQ1 - Detecting Adversarial Patch Attack

Table I shows the detection performance of *Jujutsu* on both datasets. We observe that a larger patch has a higher attack success rate as it allows more perturbations. For example, for ResNet-50 on ImageNet, a 4% patch has a success rate of about 77%, while a 6% patch has a success rate of 97%. Appendix A shows the generated patches visually.

We report the detection performance in terms of *detection success recall* on adversarial samples (which is the fraction of adversarial samples detected by *Jujutsu*) and *detection FPR* on benign inputs. Benign inputs are the same as the adversarial samples without the adversarial patch. As we use two random images from the hold-out dataset, we consider an image adversarial if the predicted label for it is identical with that of *both the hold-out images* implanted with the suspicious features. Otherwise, we consider it to be a benign input.

As shown, *Jujutsu* is able to consistently detect the adversarial samples, with a detection success recall rate of over 85% across patch sizes (in most cases). On average, it can detect over 94% of the adversarial samples on both datasets. The average FPR is 7.44% on ImageNet and 2.98% on ImageNette, and the FPR can be further reduced during the mitigation phase (see Table II).

We also find the detection success recall increases with the size of the patch. For example, for ResNet-50 on ImageNet, the detection success recall increases from about 87% for the 4% patch, to over 99% for the 6% patch. This is because a larger patch is more likely to cause misclassification on the hold-out inputs, which will be detected by *Jujutsu*. Similar trends are observed in both datasets. However, the detection FPR does not exhibit a clear trend with the patch size.

On ImageNet and ImageNette, *Jujutsu* is able to detect 93.96% and 95.51% of the adversarial samples with 7.44% and 2.98% of FPR.

C. RQ2 - Mitigating Adversarial Patch Attack

Our mitigation technique consists of a combination of parametric masking and inpainting. The resulting images after mitigation are (partially) masked and inpainted (see Fig. 2).

Metrics. We use 3 metrics for evaluation in this section.

- 1) *Robust Accuracy*: This is the prediction accuracy on the adversarial samples, and computed as follows: if *Jujutsu* detects $m\%$ of adversarial samples, and mitigates $n\%$ of the detected inputs, then the robust accuracy is $m * n\%$. We use the clean accuracy, which is the accuracy for benign inputs as a reference for comparison.
- 2) *Mitigation FPR*: This is the (reduced) FPR from the two-staged combination of detection and mitigation (explained in Section III-C3). We compare the mitigation FPR with the detection FPR to evaluate how the proposed mitigation technique can reduce the FPRs.
- 3) *Mitigation success recall*: This is the detection recall from the two-staged combination of detection and mitigation (explained in Section III-C3) - we distinguish this from the *detection success recall*, which is the detection recall from the detection technique alone. We compare the mitigation success recall with the detection success recall.

1) *Results*: We report the results of the mitigation technique in terms of aforementioned metrics in Fig. 6 (for 6% patch), Fig. 7 (for 5% patch) and Fig. 8 (for 4% patch) for each DNN on ImageNet dataset. We observe similar trends on the results from ImageNette dataset and thus we omit the detailed results. The average results on both datasets is presented in Table II.

Robust accuracy. When the masking percentage is low, the robust accuracy is low (blue straight lines in the figures) and is significantly lower than the clean accuracy (blue dash lines). This is because a large portion of the adversarial pixels are intact in the image, which continue to manipulate the output. However, with more pixels (in the suspicious features) being inpainted, the robust accuracy increases, which is because *Jujutsu* performs inpainting on more adversarial pixels. This would in turn allow the network to make a correct inference.

For most of the networks attacked by different patches, we find that by performing inpainting on 100% of the suspicious features, our mitigation technique is able to yield robust accuracy that is *comparable or higher than* the clean accuracy. The exceptions are ResNet-50 and VGG16 and ResNet-152 in Fig. 8 for the 4% patch. This is because *Jujutsu* has a (rela-

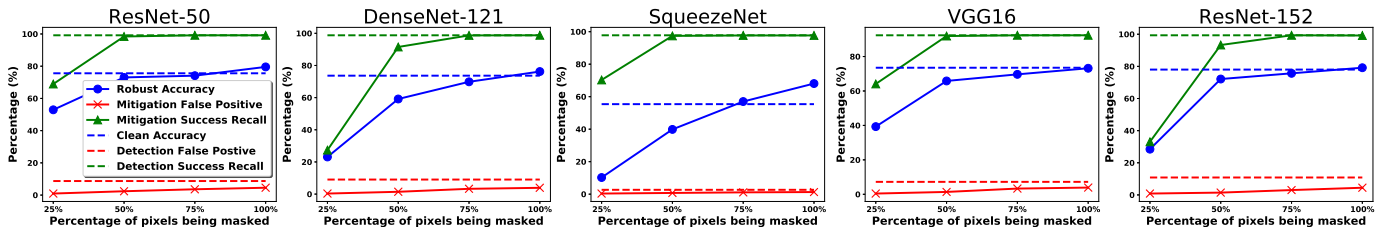


Fig. 6: Result for mitigating adversarial samples with 6% patches. (1) *Robust Accuracy* is the prediction accuracy on the adversarial samples and *Clean Accuracy* on the benign inputs. (2) *Mitigation FPR* is the FPR from the two-staged combination of detection and mitigation; and *Detection FPR* is the FPR by the detection alone. (3) *Mitigation Success Recall* is the detection recall measured from the two-staged combination of detection and mitigation; and *Detection Success Recall* is that from the detection alone. Same for Fig.7 and Fig.8.

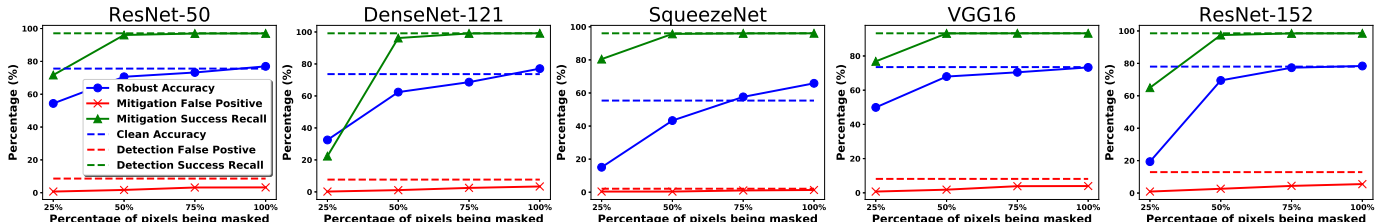


Fig. 7: Result for mitigating adversarial samples with 5% patches.

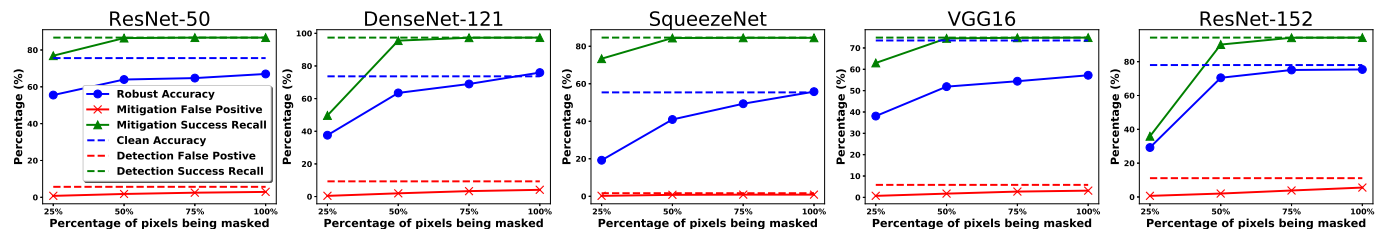


Fig. 8: Result for mitigating adversarial samples with 4% patches.

tively) low detection success recall on small patches (Column 5 in Table I). Recall that the robust accuracy is calculated from $m * n\%$, where m is the detection success recall, and n is the amount of detected images that are mitigated. We find that n is consistent across patches of different sizes, while m is lower for smaller patches. Therefore, the robust accuracy is lower on small patches.

Mitigation FPR. As shown, the mitigation FPR (red straight lines) is consistently lower than the detection FPR (red dash lines), which demonstrates the effectiveness of *Jujutsu* in reducing the FPR. The reduction in FPR is most pronounced when the masking percentage is low. This is because lower masking percentage means the inpainted image is *more likely* to resemble the original input (see Fig. 5 for an example) and thus the prediction labels on both images are *more likely* to be the same, based on which a potential FPR can be eliminated.

Mitigation success recall. When the masking percentage is low, the mitigation success recall (green straight lines) is much smaller than the detection success recall (green dash lines). This means that many of the adversarial samples that are detected as adversarial in the first phase are incorrectly flagged as benign. This is because the adversarial samples

are likely to trigger misclassification even after inpainting, when the masking percentage is low (similar to why the robust accuracy is low for 25% masking images).

On the other hand, we find that as masking percentage increases, the mitigation success recall approaches the original detection success recall. This is because with more pixels being inpainted, the likelihood of the adversarial samples to cause misclassification is low.

Comparison on using masking alone vs. masking and inpainting. To evaluate the effectiveness of image inpainting versus performing masking alone, we consider two mitigation techniques, (1) masking alone, and (2) masking with inpainting (our mitigation technique). Table II shows the results.

Robust accuracy: Masking with inpainting is able to yield higher robust accuracy than masking alone. This is because inpainting synthesizes the missing semantic contents in the mask for the network to make a correct prediction. The only exception is when only 25% of the pixels are masked, where masking alone has higher robust accuracy than masking and inpainting. This is because image inpainting relies on the regions outside the mask as the context to synthesize the contents. When the masking percentage is small, a large portion of the

TABLE II: Comparing the results from using inpainting with masking, and masking alone. Better results are highlighted in **bold**.

Metric (%)	Approach	ImageNet				ImageNette			
		Masking percentage				Masking percentage			
		25%	50%	75%	100%	25%	50%	75%	100%
Robust Accuracy	Inpainting	33.66	60.97	67.07	71.94	21.85	64.21	70.45	74.24
	Masking	43.16	60.22	64.64	70.78	28.35	62.27	66.49	71.89
Mitigation FPR	Inpainting	0.58	1.56	2.84	3.48	0.20	0.50	1.02	1.23
	Masking	1.64	2.78	3.59	3.46	0.58	1.08	1.39	1.35
Mitigation Success Recall	Inpainting	58.59	92.14	93.90	93.93	29.16	90.04	95.49	95.51
	Masking	71.85	93.37	93.92	93.94	40.02	91.89	95.51	95.51

adversarial pixels remain intact, and thus inpainting cannot reconstruct the contents correctly. In this case, it is better to mask the perturbations to shield their contributions to the prediction, rather than inpainting them.

Mitigation FPR: When comparing to masking alone, masking with inpainting achieves a lower FPR, because the benign inputs are more likely to result in the same prediction label as the inpainted inputs than inputs that are merely masked.

Mitigation success recall: While masking alone is able to achieve higher detection recall compared to masking and inpainting when the masking percentage is small, the difference becomes negligible when the masking percentage increases. This is because when the masking percentage is low, the masked images are more likely to have a label *different* from those of the original images; while the inpainted images are more likely to have the *same* label as the original image - this is similar to the reason why robust accuracy from masking alone is higher than that from masking and inpainting for 25% masking. However, when the masking percentage increases, both the masked and inpainted images are likely to be given labels different from that of the original image - thus the difference becomes negligible between both approaches.

Trade-off by varying masking percentage: Our results also show that the proposed parametric masking is able to moderate the balance between different metrics, based on which the defender can adjust *Jujutsu* to prioritize different outcomes. For instance, if the defender’s goal is to detect/mitigate adversarial attack while *minimizing* the accuracy drop on the benign inputs, she can perform image inpainting on 50% of the suspicious features, which is able to detect over 90% of the adversarial samples, achieve a robust accuracy of over 60% with a FPR of less than 2%. On the other hand, if the defender wants to *maximize Jujutsu’s* performance, she can perform image inpainting on 100% of the suspicious features, which yields the highest robust accuracy and detection success recall with a slightly higher FPR.

Our mitigation technique is able to balance between different performance metrics, by varying the percentages of masking and inpainting appropriately.

A. To *minimize* the accuracy drop on benign inputs, *Jujutsu* can detect an average of 91% of the adversarial samples, achieve an average robust accuracy of over 62% with an average FPR of 1% by performing inpainting on 50% of the suspicious features.

B. To *maximize Jujutsu’s* performance, *Jujutsu* achieves an average detection success recall of 94%, robust accuracy of 73%, and a FPR of less than 2.3% by performing inpainting on 100% of the suspicious features.

D. RQ3 - Comparison with Related Techniques

Related techniques can be divided into empirical defenses [16], [14], [12], [17], [18] and certified defenses [28], [26], [25], [27]. Empirical defenses aim to provide better empirical results while lacking provable robustness. Certified defenses can provide provable robustness but with less promising results. For instance, the leading certified defense technique, PatchGuard [25] can only achieve limited (certified) robust accuracy from 20% to 33% on ImageNet, while empirical defenses like LGS [16] and adversarial training can achieve much better (empirical) robust accuracy of over 60%. Therefore, we compare *Jujutsu* with four state-of-the-art empirical techniques, and do not consider certified defenses.

1. Localized Gradient Smoothing [16]. Naseer et al. [16] propose local gradient smoothing (LGS) to neutralize the effect of adversarial patch pixels. They first perform normalization over the gradient values, and then use a moving window to identify high-density regions (based on certain thresholds), which will be smoothed out to suppress the influence of the adversarial pixels. We use the implementation from Github [45], and set the threshold as 0.1 and smoothing factor as 2.3 as in the original paper.

2. STRIP [14]. Gao et al. [14] propose STRIP to defend against patch-like trojaned adversarial samples by superimposing the target image with a number of new images (similar to Chou et al. [12]), and detect adversarial samples based on the prediction entropy on the set of new images. The prediction entropy is compared against a detection boundary (derived from benign inputs), and a low entropy indicates that the target image is adversarial. We use the implementation from Github [46], and we use 2000 images for deriving the detection threshold and construct 100 superimposed samples per testing image, similar to the original paper.

3. Adversarial training. Adversarial training (AT) increases the robustness of DNNs by explicitly training the networks to be robust against the patch attack [17], [18].

We adapt the approach from [17], [18] to conduct AT on ImageNette. We first train the models on clean images, which is then used for adversarial training. For each DNN, we train three different models, one for each patch size. Following the best practices [47], we train the models by using the

TABLE III: Comparison with LGS [16], STRIP [14], SentiNet [12]. Better results are highlighted in **bold**.

Metric (%)	Technique			
	LGS	STRIP	SentiNet	Jujutsu
F1-Detection ¹	N/A	56.90	69.79	95.18
F1-Mitigation ²	71.03	N/A	N/A	82.02

¹ F1-detection means the F1 score is measured from detection success recall and FPR. This is for detection technique (STRIP and SentiNet).

² F1-mitigation means the F1 score is measured from robust accuracy and FPR. This is for mitigation technique (LGS).

SGD optimizer and varying different hyperparameters such as learning rate, momentum, dropout, number of epochs, batch size (more details in Appendix C).

4. SentiNet [12]. Chou et al. [12] propose SentiNet for detecting the patch attack. SentiNet first uses a selective search image segmentation to generate a list of class proposals, i.e., input segments corresponding to different classes. It then extracts the salient maps from the class proposals and identifies the unique salient features, by subtracting the common regions in the saliency maps, which is then overlaid to a set of new images. Finally, it distinguishes adversarial and benign features by replacing the salient features with inert patterns such as Gaussian noise. It considers the salient features to be adversarial if (1) the number of images misclassified is high, and (2) the average confidence values from images with inert patterns is high. SentiNet [12] is the most closely related to *Jujutsu*. We describe the qualitative difference between *Jujutsu* and SentiNet in Section V. We focus on quantitative comparison in this section. We use the implementation from Lovisotto et al. [48]. We follow Chou et al. [12] to overlay the salient features from the test image to 100 new images, which is to calculate the statistics for detecting adversarial samples. We randomly sample 400 clean images to compute the detection threshold for detection.

Comparison Metric. To evaluate each technique’s performance on adversarial and benign samples, we report the *F1 score* for each technique, which is the harmonic mean of the precision and recall (higher values are better). Precision indicates the ratio of adversarial samples that are detected or mitigated by the technique among all the (adversarial and benign) samples detected or mitigated. Recall indicates the ratio of adversarial samples that are detected or mitigated by the technique among all the adversarial samples.

Comparison with LGS, STRIP and SentiNet.

We compare *Jujutsu* (using 100% masking with inpainting, which yields the highest robust accuracy) with LGS, STRIP and SentiNet on ImageNet in Table III. For each technique, we consider all 5 DNNs, each of which is evaluated on patches in all sizes (4%, 5% and 6%). We show the average results in Table III, which shows that *Jujutsu* has significantly higher F1 scores for detection and mitigation than the other techniques. We explain the reasons behind each technique’s poor performance in Section V.

Comparison with adversarial training (AT). The best F1 score yielded by AT under different settings (recall there are 3

TABLE IV: Comparison with AT in defending against *multiple* targeted classes. Better results are highlighted in **bold**.

F1-Mitigation (%)	Number of target classes		
	1 target	3 targets	5 targets
Adversarial Training	83.10	71.09	65.43
Jujutsu	90.66	86.48	84.99

models trained with 4%, 5% and 6% patches) is 82.32, which is slightly lower than 84.95 achieved by *Jujutsu*. The detailed results are in Table XI in Appendix C.

A main disadvantage of AT is that it requires training for *each* class, which is challenging for attacks targeting diverse classes. In contrast, *Jujutsu* does not require any training, and is agnostic to the target classes determined by the attacker, which makes it more scalable. To validate this, we perform a targeted experiment to evaluate patch attack targeting *multiple* labels, and we compare AT with *Jujutsu*. We choose ResNet-50 with 6% patch. For AT with multiple targets, each training batch contains adversarial samples targeting different classes.

We report the results in Table IV. As can be seen, the gap between *Jujutsu*’s performance and AT’s performance increases as the number of target classes increases, with *Jujutsu* outperforming AT considerably as the number of classes increases. The F1 score by *Jujutsu* is 7% higher than that by AT for 1-target patch attack, and this difference becomes ~20% when the number of target classes increases to 5. AT’s performance degrades quickly because as the number of target classes increases, the learning objective becomes increasingly difficult for adversarial training - this is similar to how common DNNs would yield lower accuracy on a 1000-class dataset than on a simple 10-class dataset.

Jujutsu significantly outperforms the state-of-art techniques LGS, STRIP, SentiNet, and adversarial training.

E. RQ4 - Defending Against Physical Patch Attack

We now evaluate the effectiveness of *Jujutsu* against adversarial patch attack in the real world. We use the printable adversarial patch from [7]. We printed it out, placed it next to the the cell phone object (a iPhone 6s device) at various locations, and captured a video of it.

We use ResNet-50 model because we find the printable patch is most effective on this model with 80.3% attack success rate. In contrast, the attack success rates on the other 4 models range from 2.5% to 48.1% (19.7% on average). We increase the length of the detection box to 142 as the physical patch occupies more pixels in the images than digital patch, in order to survive under the camera transformation [7].

Fig. 9 shows the video frames in our evaluation. Both videos with and without patches contain around 430 frames. 80% of the frames with patches successfully caused the targeted misclassification. All the frames without patches are correctly classified as “cellphone” or “iPod” (the device can be interpreted as either a cellphone or an iPod device).

As before, we evaluate the effectiveness of the proposed technique (using masking and image inpainting) in terms of



Fig. 9: Video frames for a cell phone object with (top row) and without (bottom row) a print-out adversarial patch.

TABLE V: Results for mitigating *physical patch attack*.

Metric (%)	Masking percentage			
	25%	50%	75%	100%
Robust Accuracy	82.46	95.32	93.86	81.87
Mitigation FPR	1.15	2.99	3.45	5.52
Mitigation Success Recall	86.84	95.91	95.91	95.91

robust accuracy, mitigation success recall as well as mitigation FPR. The results are shown in Table V.

Robust accuracy. Unlike the previous evaluation on digital patch, we can see from Table V that a low masking percentage is able to yield a high robust accuracy for the physical attack (this is low for the evaluation on digital patch). This is because the perturbations in the physical patch are more susceptible to masking and inpainting compared with the digital patch that is directly applied to the image. Perturbations in the physical patch need to undergo camera transformation, which makes the perturbations more amenable to being mitigated by *Jujutsu*. Thus, even a low masking percentage in *Jujutsu* is able to effectively mitigate the physical patch attack.

In addition, the robust accuracy from 75% and 100% masking is lower than that from 50%, which is unlike the trend in the previous evaluation for digital patch. This is because the detection box is larger, and hence higher masking percentage means a lot of pixels in the images are masked for inpainting. The quality of the inpainted image degrades when the masking area is large, and thus the network is not able to infer correct label from the inpainted image. In contrast, 50% masking yields the highest robust accuracy of 95.32%.

Mitigation FPR. *Jujutsu* yields a FPR ranging from 1.15% to 5.52%. Similar to the digital patch, the FPR is higher when the masking percentage is higher.

Mitigation success recall. *Jujutsu* yields a mitigation success recall ranging from 86.84% to 95.91%. The trend is similar to that for the digital patch, i.e., the success recall is low when the masking percentage is low, and high otherwise.

For physical patch attack, *Jujutsu* has a detection accuracy of 95.91%, robust accuracy of 95.32% on adversarial samples, and a FPR of 2.99% by masking and inpainting 50% of the suspicious features.

F. RQ5 - Attacks Targeting Different Labels

This section evaluates *Jujutsu* against attacks that target different class labels. For each target label, we need to perform training to generate the universal adversarial patches and the

TABLE VI: Results on mitigating *attacks that target 5 different labels*.

Metric (%)	ImageNet	ImageNette	Average
Robust Accuracy	76.33	74.49	75.41
Mitigation FPR	2.24	0.8	1.52
Mitigation Success Recall	96.47	90.77	93.62



Fig. 10: An illustration of adversarial patches in different shapes.

training of adversarial patch is time-consuming. Hence, we train five 6% patches that target different labels for each dataset using ResNet-50. Note that training is only needed for creating the adversarial patches and *Jujutsu* does not require any training.

Table VI shows the results. We find that *Jujutsu* is able to consistently achieve high performance in detecting and mitigating patch attacks targeting different labels, and with very low FPR. On average, *Jujutsu* detects over 93% of the adversarial samples, achieves a robust accuracy of over 75% with 1.5% FPR. This high accuracy is because *Jujutsu* works by comparing the prediction label before and after feature transplantation, which is *agnostic* to the exact target label.

Jujutsu is able to defend against attacks targeting diverse labels with high performance and low FPR.

G. RQ6 - Attacks with Different Patch Shapes

We consider adversarial patches in three different shapes: square, circle and rectangle, as shown in Fig. 10. Table II evaluated *square* adversarial patches (which is our default setting) and Table V evaluated *circular* patches. We now describe the evaluation on *rectangular* patches, and then summarize the results for patches in all three different shapes.

We train the rectangular patches on all five models on both datasets, and consider patches in different sizes. We change the square bounding box to a rectangular one, which occupies around 20% of pixels as the square bounding box. Note that we do not know the exact width/height ratio of the rectangular shape created by the attacker (patch sizes are given in Table VII). Our detection bounding box has a width/height ratio of 6:4. We show in Table VII the results for defending against rectangular patches in various sizes. As shown, *Jujutsu* is able to achieve high detection and mitigation performance on rectangular patches with a very low FPR.

We summarize *Jujutsu*'s performance on all three patches in Table VIII. On average, *Jujutsu* is able to detect over 95% of adversarial patches in different shapes, achieve a robust accuracy of over 80% with 2.33% FPR.

Jujutsu is able to defend against attacks with different patch shapes with high performance and low FPR.

TABLE VII: Results for defending against attacks using rectangular patch.

Metric (%)	ImageNet			ImageNette		
	Patch size			Patch size		
	30*70	33*80	36*88	30*70	33*80	36*88
Robust Accuracy	67.27	72.09	71.37	74.43	74.62	74.92
Mitigation FPR	1.64	1.62	1.54	1.59	1.74	1.65
Mitigation Succ. Recall	89.91	95.54	97.24	97.54	99.07	99.19

H. RQ7 - Adaptive Attack

We evaluate the robustness of *Jujutsu* against two adaptive attacks that are aware of *Jujutsu* and attempt to bypass it by either (1) evading the detection mechanism; or (2) evading the mitigation technique *even if they are detected*. We consider the ImageNet dataset.

1) *Evading the Detection*: We consider an adaptive attack to evade the detection by reducing the influence of the adversarial patch on the final prediction so that the patch will not be identified as salient (i.e., suspicious) features.

Attack setup. The influence on the final prediction is derived from the saliency map. Thus the attacker’s goal is to manipulate the saliency map such that the regions of the adversarial patch will not become salient. This attack can be formulated as the following objective function during the generation of the adversarial patch:

$$\delta = \underset{\delta}{\operatorname{argmax}} \mathbb{E}_{x \sim X, l \sim L} (\log \Pr(y = y^{adv} | x') - \|\hat{M}_j^*(x) - m_0^*\|_2^2), \quad (5)$$

where $\hat{M}_j^*(x)$ is defined as the saliency map on the region where the adversarial patch resides (not the entire saliency map), and m_0^* is a mask in the same size of the adversarial patch and filled with 0. The first term’s goal is to cause targeted misclassification, while the second term’s goal is to let $\hat{M}_j^*(x)$ have *small* influence, by forcing the values within $\hat{M}_j^*(x)$ to be close to 0. The closer $\hat{M}_j^*(x)$ is to 0, the more likely is the resulting patch δ to evade detection.

The second term can be viewed as manipulating the Hessian matrix of $F(x)$, which is all zero for DNNs with ReLU activation functions [49], [50]. Therefore, we replace the ReLU function with its smooth approximation when calculating the gradients. Following the approach in prior work [50], [51], we choose a parametric softplus function which is differentiable for the second-order derivative. The parametric softplus function can be expressed as: $f(x) = \frac{1}{\alpha} \log(1 + \exp(\alpha x))$, where x is the original input to the ReLU function, and α is the hyperparameter to control the shape of the curve. We follow Xie et al. [51] to empirically set α as 10 in our experiment. Finally, we only use the parametric softplus for backward propagation, and use ReLU for the normal forward pass.

To be conservative, we consider the 6% patch, which allows the attacker to inject larger number of perturbations to evade *Jujutsu*. We choose 200 samples for training the adversarial patch, 500 steps per sample and 20 epochs in total.

Equation 5 requires several forward and backward passes for calculating the saliency map $\hat{M}_j^*(x)$, which is much more time-consuming than the original optimization (Equation 3). Therefore, we reduce the sampling size n in Equation 4 from

TABLE VIII: Summary for defending against attacks using different patches.

Metric (%)	Patch shape			Avg.
	Square	Circle	Rectangular	
Robust Accuracy	73.09	95.32	72.45	80.29
Mitigation FPR	2.36	2.99	1.63	2.33
Mitigation Succ. Recall	94.72	95.91	96.41	95.68

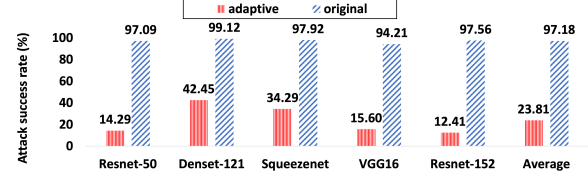


Fig. 11: Attack success rate for adaptive attack to evade the detection. The higher the better.

50 to 5 for faster training. We experimentally verified that the smaller sampling size n does not significantly affect the resulting saliency map, and that we can still find all the salient features. Under this setting, it took around 10 days to generate an adversarial patch on ResNet-152, compared to about 300 days if we had followed our previous setup in Section IV-A2.

Result. We compare the attack success rate of the patches generated from both the original and adaptive attackers in Fig. 11. As shown, the attack success rate is degraded from 97.18% to 23.81% for the adaptive attacker who attempts to evade detection. This is because in Equation 5, the first term aims to *increase* the influence on the final prediction such that the output label can be manipulated; while the second term *reduces* the influence on the output. This equation constrains the adaptive attacker, who cannot evade detection without also significantly degrading the attack’s effectiveness.

While *Jujutsu*’s detection performance in this case degrades because the resulting adversarial patches have lower attack success rates (detailed detection evaluation is in Appendix D), *Jujutsu* is able to significantly limit the attacker’s capability to generate universal adversarial patch. With *Jujutsu*, the adversarial patches generated by adaptive attacker are much more likely to *fail* to fool the DNNs, which means the DNNs are *significantly less susceptible* to patch attack.

2) *Evading the Mitigation*: We consider an adaptive attacker who attempts to cause targeted misclassification even if the adversarial samples are detected. Because our masking strategy is parametric, the adaptive attack would be unsuccessful if we mask the entire set of suspicious features and perform image inpainting since all of the adversarial perturbations would be removed. Therefore, we study whether the adaptive attack could succeed if we mask only 50% or 75% of the suspicious features.

Attack setup. To model the masking of $x\%$ of the suspicious features, we randomly set $x\%$ of the values that are non-zero within the mask $m \in \{0, 1\}^n$ to be 0, so that those positions marked with a 0 will not be available for manipulation by the attacker. The attacker, thus has to use only the remaining perturbations to cause misclassification.

Similar to Section IV-H1, we consider the 6% patch to

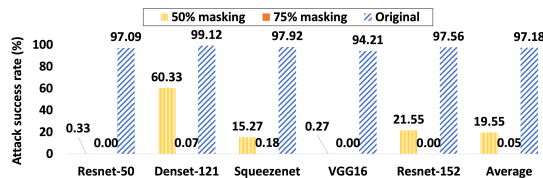


Fig. 12: Attack success rate for adaptive attack to evade the mitigation. The higher the better.

maximize the attack’s influence. For the masking percentage of 50%, we use 2000 images, a maximal step of 1000 and 30 epochs in total, which is in line with our standard attack generation as in Section IV-A2. This is because evading the mitigation does not require several forward and backward passes for each step as in Section IV-H1, and thus we can use more images and optimization steps as well as epochs.

For the masking percentage of 75%, we use a maximal epoch of 20, because our evaluation shows that the training is not able to make any progress, and the attack success rate is consistently close to 0%. We plot the training progress for each network in Appendix E.

Result. Fig. 11 shows the results. As in the case of the detection, we see that the patches generated from the adaptive attack suffer from significant effectiveness drop despite them attempting to avoid being mitigated. For the masking percentage of 50%, the average attack success rate is degraded from 97.18% to 19.55%, while for the masking percentage of 75%, it is degraded from 97.18% to 0.05%. The attack success rate for the 50% masking is higher than that for the 75% masking because more perturbations remain after masking in the former case, which are likely to cause misclassification. When 75% of the perturbations are masked, it is almost impossible for the attacker to generate an adversarial patch that evades the mitigation, and hence the success rate is near 0%. This means adaptive attack is most likely to be unsuccessful in attacking the DNNs with the protection of *Jujutsu*.

Jujutsu is able to make the DNNs significantly less susceptible to patch attack under adaptive attacks.

V. RELATED WORK

Defense against adversarial attack can be divided into certified [28], [26], [25], [27] and practical defense [16], [19], [17], [18], [15], [13], [14], [12]. *Jujutsu* is a practical defense and thus here we mainly focus on related practical defenses.

Naseer et al. [16] propose local gradient smoothing (LGS) to mitigate patch attack by identifying the regions with high gradient magnitude and neutralizing the gradients of those regions whose values are greater than a certain threshold. This method could fail because neutralizing the gradient magnitude of adversarial pixels does not guarantee the network to make correct prediction on the resulting image and benign pixels could also have high gradient magnitude (thus LGS achieves a high FPR). Our evaluation shows that *Jujutsu* significantly outperforms LGS in both robust accuracy and FPR.

Hayes et al. [19] generate saliency maps to detect and remove adversarial pixels based on pre-defined thresholds to

scan the saliency map. Jha et al. [15] propose to selectively mask the top-k% salient features based on the saliency map to remove the adversarial effects. Ma et al. [13] propose to detect patch-like adversarial sample based on invariant checking. While useful in defending against patch attack, these techniques suffer from high FPRs (from 14.97% [13] to over 30% [15]). In contrast, *Jujutsu* yields an average FP of less than 3% with high defense performance.

Adversarial training (AT) is also used to defend against patch attack [17], [18]. Our quantitative comparison with AT in Section IV-D shows that *Jujutsu* outperforms AT, especially when defending against attacks that target multiple labels.

Gao et al. [14] propose STRIP to detect patch-like trojaned adversarial samples by superimposing the target image with a set of new images and measuring the prediction entropy on the set of new images. STRIP achieves low detection performance because the adversarial patch is no longer effective after being blended with the new images, thus the prediction entropy is high on the new images.

Chou et al. [12] propose SentiNet for detecting patch attack based on statistical analysis. There are 4 qualitative differences between *Jujutsu* and SentiNet. (1) While both SentiNet and *Jujutsu* involve transplanting salient features to new images, SentiNet extracts the unique suspicious features by subtracting the common regions of the saliency maps belonging to different classes. However, this approach is *problematic* when the adversarial patch occurs in the common regions of the saliency maps belonging to different classes. This is because the regions associated with adversarial patch will be removed after subtraction. Thus SentiNet will fail to locate the adversarial patch (our evaluation in Section IV-D validates this). In contrast, *Jujutsu* identifies suspicious features by preprocessing the saliency map and drawing a bounding box to locate the unique suspicious features. (2) SentiNet transplants the salient features to a *random* region of an image and hence this could cause FPR when the salient features override the image’s natural features. *Jujutsu* instead resolves this problem by specifically transplanting the salient features to the *least-salient* region of the image. As a result, we find that *Jujutsu* achieves a much lower FPR (31% lower than SentiNet). (3) SentiNet performs detection by statistical analysis while *Jujutsu* detects adversarial samples by prediction consistency - our results show that *Jujutsu* detects significantly more adversarial samples than SentiNet (67% more than SentiNet). The reason behind SentiNet’s poor detection performance is that it is not able to reliably locate the adversarial patch, and thus fails in the subsequent analysis. (4) SentiNet only offers attack detection but not any mitigation for the attack. In contrast, *Jujutsu* offers both detection and mitigation, which is more desirable as it enables automated recovery from attacks.

VI. CONCLUSION

This work proposes *Jujutsu*, a technique to detect and mitigate robust and universal adversarial patch attack against image classification DNNs. For detection, we exploit the universal nature of the patch attack by using explainable AI

techniques to identify features that are potentially malicious. We determine the maliciousness of the suspicious features by transplanting the features to two new hold-out images, and comparing the prediction labels on both images. For mitigation, we leverage the localized nature of the patch attack. We propose a parametric masking strategy to shield the output from malicious perturbations. To allow the DNNs to correctly classify the corrupted input, we use image inpainting to synthesize alternative contents in the regions that are overridden by the adversarial perturbations and generate a “clean” image.

Our evaluation on five popular DNNs and two datasets shows that *Jujutsu*: (1) achieves superior detection and mitigation performance and significantly outperforms existing techniques; (2) can defend against physical-world attack; (3) can defend against attacks that use patches in various shapes; (4) can defend against attacks that target diverse classes; (5) makes the DNNs significantly less susceptible to patch attack under adaptive attacks.

REFERENCES

- [1] C. Szegedy, W. Zaremba, I. Sutskever, J. Bruna, D. Erhan, I. Goodfellow, and R. Fergus, “Intriguing properties of neural networks,” *arXiv preprint arXiv:1312.6199*, 2013.
- [2] L. Huang, C. Gao, Y. Zhou, C. Xie, A. L. Yuille, C. Zou, and N. Liu, “Universal physical camouflage attacks on object detectors,” in *Proceedings of the IEEE/CVF Conference on Computer Vision and Pattern Recognition*, 2020, pp. 720–729.
- [3] Z. Li, Y. Wu, J. Liu, Y. Chen, and B. Yuan, “Advpulse: Universal, synchronization-free, and targeted audio adversarial attacks via subsecond perturbations,” in *Proceedings of the 2020 ACM SIGSAC Conference on Computer and Communications Security*, 2020, pp. 1121–1134.
- [4] P. Neekhara, S. Hussain, P. Pandey, S. Dubnov, J. McAuley, and F. Koushanfar, “Universal adversarial perturbations for speech recognition systems,” *arXiv preprint arXiv:1905.03828*, 2019.
- [5] L. Song, X. Yu, H.-T. Peng, and K. Narasimhan, “Universal adversarial attacks with natural triggers for text classification,” *arXiv preprint arXiv:2005.00174*, 2020.
- [6] E. Wallace, S. Feng, N. Kandpal, M. Gardner, and S. Singh, “Universal adversarial triggers for attacking and analyzing nlp,” *arXiv preprint arXiv:1908.07125*, 2019.
- [7] T. B. Brown, D. Mané, A. Roy, M. Abadi, and J. Gilmer, “Adversarial patch,” *arXiv preprint arXiv:1712.09665*, 2017.
- [8] S.-M. Moosavi-Dezfooli, A. Fawzi, O. Fawzi, and P. Frossard, “Universal adversarial perturbations,” in *Proceedings of the IEEE conference on computer vision and pattern recognition*, 2017, pp. 1765–1773.
- [9] K. Eykholt, I. Evtimov, E. Fernandes, B. Li, A. Rahmati, C. Xiao, A. Prakash, T. Kohno, and D. Song, “Robust physical-world attacks on deep learning visual classification,” in *Proceedings of the IEEE Conference on Computer Vision and Pattern Recognition*, 2018, pp. 1625–1634.
- [10] A. Athalye, L. Engstrom, A. Ilyas, and K. Kwok, “Synthesizing robust adversarial examples,” in *International conference on machine learning*. PMLR, 2018, pp. 284–293.
- [11] R. Feng, J. Chen, N. Manohar, E. Fernandes, S. Jha, and A. Prakash, “Query-efficient physical hard-label attacks on deep learning visual classification,” *arXiv preprint arXiv:2002.07088*, 2020.
- [12] E. Chou, F. Tramer, and G. Pellegrino, “Sentinet: Detecting localized universal attacks against deep learning systems,” in *2020 IEEE Security and Privacy Workshops (SPW)*. IEEE, 2020, pp. 48–54.
- [13] S. Ma, Y. Liu, G. Tao, W. Lee, and X. Zhang, “Nic: Detecting adversarial samples with neural network invariant checking,” in *NDSS*, 2019.
- [14] Y. Gao, C. Xu, D. Wang, S. Chen, D. C. Ranasinghe, and S. Nepal, “Strip: A defence against trojan attacks on deep neural networks,” in *Proceedings of the 35th Annual Computer Security Applications Conference*, 2019, pp. 113–125.
- [15] S. Jha, S. Raj, S. L. Fernandes, S. K. Jha, S. Jha, G. Verma, B. Jalaian, and A. Swami, “Attribution-driven causal analysis for detection of adversarial examples,” *arXiv preprint arXiv:1903.05821*, 2019.
- [16] M. Naseer, S. Khan, and F. Porikli, “Local gradients smoothing: Defense against localized adversarial attacks,” in *2019 IEEE Winter Conference on Applications of Computer Vision (WACV)*. IEEE, 2019, pp. 1300–1307.
- [17] S. Rao, D. Stutz, and B. Schiele, “Adversarial training against location-optimized adversarial patches,” *arXiv preprint arXiv:2005.02313*, 2020.
- [18] T. Wu, L. Tong, and Y. Vorobeychik, “Defending against physically realizable attacks on image classification,” in *International Conference on Learning Representations*, 2020.
- [19] J. Hayes, “On visible adversarial perturbations & digital watermarking,” in *Proceedings of the IEEE Conference on Computer Vision and Pattern Recognition Workshops*, 2018, pp. 1597–1604.
- [20] D. Smilkov, N. Thorat, B. Kim, F. Viégas, and M. Wattenberg, “Smoothgrad: removing noise by adding noise,” *arXiv preprint arXiv:1706.03825*, 2017.
- [21] M. Ancona, E. Ceolini, C. Öztireli, and M. Gross, “Towards better understanding of gradient-based attribution methods for deep neural networks,” *arXiv preprint arXiv:1711.06104*, 2017.
- [22] R. R. Selvaraju, M. Cogswell, A. Das, R. Vedantam, D. Parikh, and D. Batra, “Grad-cam: Visual explanations from deep networks via gradient-based localization,” in *Proceedings of the IEEE international conference on computer vision*, 2017, pp. 618–626.
- [23] D. Karmon, D. Zoran, and Y. Goldberg, “Lavan: Localized and visible adversarial noise,” *arXiv preprint arXiv:1801.02608*, 2018.
- [24] S. Abdoli, L. G. Hafemann, J. Rony, I. B. Ayed, P. Cardinal, and A. L. Koerich, “Universal adversarial audio perturbations,” *arXiv preprint arXiv:1908.03173*, 2019.
- [25] C. Xiang, A. N. Bhagoji, V. Schwag, and P. Mittal, “Patchguard: Provable defense against adversarial patches using masks on small receptive fields,” *arXiv preprint arXiv:2005.10884*, 2020.
- [26] A. Levine and S. Feizi, “(de) randomized smoothing for certifiable defense against patch attacks,” *arXiv preprint arXiv:2002.10733*, 2020.
- [27] M. McCoyd, W. Park, S. Chen, N. Shah, R. Roggenkemper, M. Hwang, J. X. Liu, and D. Wagner, “Minority reports defense: Defending against adversarial patches,” *arXiv preprint arXiv:2004.13799*, 2020.
- [28] P.-y. Chiang, R. Ni, A. Abdelkader, C. Zhu, C. Studor, and T. Goldstein, “Certified defenses for adversarial patches,” *arXiv preprint arXiv:2003.06693*, 2020.
- [29] J. Lu, H. Sibai, E. Fabry, and D. Forsyth, “No need to worry about adversarial examples in object detection in autonomous vehicles,” *arXiv preprint arXiv:1707.03501*, 2017.
- [30] J. Yu, Z. Lin, J. Yang, X. Shen, X. Lu, and T. S. Huang, “Free-form image inpainting with gated convolution,” in *Proceedings of the IEEE International Conference on Computer Vision*, 2019, pp. 4471–4480.
- [31] G. Liu, F. A. Reda, K. J. Shih, T.-C. Wang, A. Tao, and B. Catanzaro, “Image inpainting for irregular holes using partial convolutions,” in *Proceedings of the European Conference on Computer Vision (ECCV)*, 2018, pp. 85–100.
- [32] C. Zheng, T.-J. Cham, and J. Cai, “Pluralistic image completion,” in *Proceedings of the IEEE Conference on Computer Vision and Pattern Recognition*, 2019, pp. 1438–1447.
- [33] M. Sundararajan, A. Taly, and Q. Yan, “Axiomatic attribution for deep networks,” *arXiv preprint arXiv:1703.01365*, 2017.
- [34] D. Pathak, P. Krahenbuhl, J. Donahue, T. Darrell, and A. A. Efros, “Context encoders: Feature learning by inpainting,” in *Proceedings of the IEEE conference on computer vision and pattern recognition*, 2016, pp. 2536–2544.
- [35] “Installing pytorch and torchvision,” <https://pytorch.org/get-started/previous-versions/>.
- [36] “Imagenet dataset,” <http://www.image-net.org/challenges/LSVRC/2012/>.
- [37] “Imagenette dataset,” <https://github.com/fastai/imagenette>.
- [38] K. He, X. Zhang, S. Ren, and J. Sun, “Deep residual learning for image recognition,” in *Proceedings of the IEEE conference on computer vision and pattern recognition*, 2016, pp. 770–778.
- [39] K. Simonyan and A. Zisserman, “Very deep convolutional networks for large-scale image recognition,” *arXiv preprint arXiv:1409.1556*, 2014.
- [40] G. Huang, Z. Liu, L. Van Der Maaten, and K. Q. Weinberger, “Densely connected convolutional networks,” in *Proceedings of the IEEE conference on computer vision and pattern recognition*, 2017, pp. 4700–4708.
- [41] F. N. Iandola, S. Han, M. W. Moskewicz, K. Ashraf, W. J. Dally, and K. Keutzer, “Squeezenet: Alexnet-level accuracy with 50x fewer parameters and 0.5 mb model size,” *arXiv preprint arXiv:1602.07360*, 2016.

- [42] “Code for adversarial patch attack,” https://github.com/A-LinCui/Adversarial_Patch_Attack.
- [43] “Pytorch implementation of smoothgrad,” <https://github.com/hs2k/pytorch-smoothgrad>.
- [44] “Code for pluristic inpainting,” <https://github.com/lyndonzheng/Pluralistic-Inpainting>.
- [45] “Code for local gradient smoothing defense,” https://github.com/metallurk/local_gradients_smoothing.
- [46] “Code for strip defense,” <https://github.com/garrisonsys/STRIP>.
- [47] “Fine-tuning torchvision model,” https://pytorch.org/tutorials/beginner/finetuning_torchvision_models_tutorial.html.
- [48] G. Lovisotto, H. Turner, I. Sluganovic, M. Strohmeier, and I. Martinovic, “SLAP: improving physical adversarial examples with short-lived adversarial perturbations,” *CoRR*, vol. abs/2007.04137, 2020. [Online]. Available: <https://arxiv.org/abs/2007.04137>
- [49] X. Zhang, N. Wang, H. Shen, S. Ji, X. Luo, and T. Wang, “Interpretable deep learning under fire,” in *29th {USENIX} Security Symposium ({USENIX} Security 20)*, 2020.
- [50] A. Ghorbani, A. Abid, and J. Zou, “Interpretation of neural networks is fragile,” in *Proceedings of the AAAI Conference on Artificial Intelligence*, vol. 33, 2019, pp. 3681–3688.
- [51] C. Xie, M. Tan, B. Gong, A. Yuille, and Q. V. Le, “Smooth adversarial training,” *arXiv preprint arXiv:2006.14536*, 2020.

APPENDIX

A. Visualization of the Adversarial Patches

We show the visulizaion of the square adversarial patches in Fig. 13 (for 6% patch), Fig. 14 (for 5% patch) and Fig. 15 (for 4% patch). We show the rectangular patches in Fig. 16, Fig. 17 and Fig. 18.



Fig. 13: Visualization of the 6% square adversarial patch (54*54*3) on ImageNet. From left to right: ResNet-50, DenseNet-121, SqueezeNet, VGG16 and ResNet-152. Same for Fig. 14 and Fig. 15.



Fig. 14: Visualization of the 5% adversarial patch (50*50*3).



Fig. 15: Visualization of the 4% adversarial patch (44*44*3).



Fig. 16: Visualization of the 6% rectangular adversarial patch (36*88*3) on ImageNet. From left to right: ResNet-50, DenseNet-121, SqueezeNet, VGG16 and ResNet-152. Same for Fig. 17 and Fig. 18.



Fig. 17: Visualization of the 5% adversarial patch (38*80*3).



Fig. 18: Visualization of the 4% adversarial patch (30*70*3).

B. Results on Using Different Number of Images for Detection

This section shows *Jujutsu*'s performance when using different number of hold-out images for attack detection. We consider 1-3 different images for all 5 DNNs on the ImageNet dataset. The results are presented in Table IX.

As shown, detection success recall reduces as the number of images for detection increases. This is because *Jujutsu* determines an adversarial sample only if *all* the images implanted with the salient features have the same labels as the original test image. When more images are used for detection, it is more difficult for the adversarial patch to cause the same misclassification on all the hold-out images (it is easier to cause the targeted misclassification on 1 image than on 2 images or more). Hence, *Jujutsu*'s detection performance degrades when more images are used for detection.

We also observe that the FPR reduces as we use more images for detection. The reason is similar to the above. Specifically, a benign image will be mis-detected only if its salient features cause the same prediction labels on all the hold-out images after feature transplantation, which is increasingly difficult as the number of hold-out images increase.

Based on the above, different number of hold-out images can be used based on different objectives, e.g., one can use more images for detection in order to minimize FP. We use 2 images for detection in our evaluation to balance detection performance and FP.

C. Additional Details on Adversarial Training

1) *Model training*: We start with training the models from scratch using ImageNette [37] training set. Following the best practices [47], we trained the models with varying hyperparameters such as learning rate from 0.001 to 0.1, momentum from 0.7 to 0.9, number of epochs from 15 to 50, batch size = 128, and used SGD optimizer. We did this for training the models from benign samples and for adversarial training. We selected the models that yield the best accuracy among different hyperparameters.

We perform adversarial training on the models that are trained from the ImageNette dataset. In each epoch during AT, we train the model using a mixture of adversarial and benign samples. To generate the adversarial samples, we first perform optimization shown in Equation 3 to construct the adversarial patch, which is then overlaid to benign samples for creating adversarial samples.

2) *Attack generation*: The attack generation follows the implementation from [42] to set epoch = 30, learning rate = 1.0, batch size = 128. We set the attack label as 'french

TABLE IX: *Jujutsu*'s performance when using different number of hold-out images for detection.

Metric (%)	Num of images for detection		
	1	2	3
Detection Success Recall	96.23%	93.96%	91.67%
Detection FPR	17.15%	7.44%	4.33%

TABLE X: Results on robust accuracy on adversarial samples; and FPR on benign inputs for each robust model trained from adversarial training.

Robust Model	Patch Size	Robust Accuracy	FPR
ResNet-50	6%	80.31%	12.98%
	5%	80.24%	13.76%
	4%	81.50%	13.4%
DenseNet-121	6%	77.70%	15.24%
	5%	76.73%	14.38%
	4%	76.92%	13.29%
SqueezeNet	6%	84.74%	13.49%
	5%	85.05%	12.47%
	4%	85.78%	12.29%
VGG16	6%	64.07%	12.79%
	5%	64.69%	11.05%
	4%	65.21%	11.16%
ResNet-152	6%	82.73%	11.79%
	5%	82.95%	11.37%
	4%	83.29%	11.23%

horn/horn' in ImageNette, which is equivalent to class 566 in ImageNet (ImageNette is a 10-class subset of ImageNet dataset).

As before, we warmstart each epoch with the patch generated from previous epoch, which is to make the patch universally adversarial. At the end of each epoch, we overlay the adversarial patch to the clean images from the validation set to create adversarial samples. We then measure the models' robust accuracy on these adversarial samples. Finally, we choose the models with the highest robust accuracy among all epochs.

3) *Detailed results*: We report the robust accuracy and FPR (i.e., the number of benign images that are misclassified by the robust models) in Table X. To evaluate the robust accuracy, we first create new adversarial patches separated from those during AT, and apply the new patches to 2000 samples as before. The adversarial patches yield attack success rate of 80-99%.

Table XI shows the comparison with AT and *Jujutsu* on the attack that targets a single class, which demonstrates that *Jujutsu* achieves the highest F1 score compared with AT. Our evaluation in Table IV further shows that the outperformance of *Jujutsu* over AT increases when the attack is targeting multiple classes (instead of a single class).

D. Detection performance on the adaptive adversarial attack in Section IV-H1

This section reports the detection performance on the adversarial patch generated from the adaptive attack that aims to evade *Jujutsu*. The results are presented in Fig. 19, and *Jujutsu* detects an average of 26.40% of the adversarial samples. This is because the adversarial patches are no longer universally adversarial, and thus they often fail to cause misclassification

TABLE XI: Comparison with Adversarial Training (AT) on defending attack targeting single class. *4%-AT* indicates the model adversarially-trained with 4% patches. *Each* technique (4%-, 5%-, 6%-AT) is evaluated on adversarial samples in *all* sizes (4%, 5% and 6% patches). Better results are highlighted in **bold**.

Metric (%)	technique			
	4%-AT	5%-AT	6%-AT	<i>Jujutsu</i>
Robust Accuracy	78.54	77.93	77.91	74.74
FPR	12.27	12.61	13.26	1.23
F1-mitigation	82.32	81.08	81.51	84.95

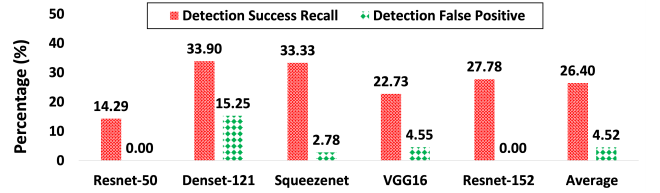


Fig. 19: Detection performance on the adversarial patch from adaptive attack that attempts to evade the detection.

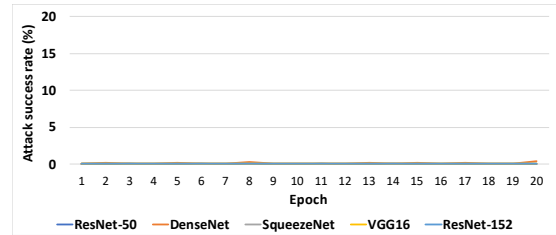


Fig. 20: Training progress for the adversarial patch when 75% of the patch are masked.

when being transplanted to hold-out inputs. As a consequence, *Jujutsu* cannot detect them as adversarial.

Nevertheless, *Jujutsu* is able to greatly reduce the attack success rate from 97.18% to 23.81%, which is able to make the DNNs much less susceptible to patch attack.

E. Visualizing the Training Progress of Adaptive Attack to Evade Mitigation

This section plots the attack success rate of the adversarial patch at each epoch during training while 75% of the adversarial pixels are masked.

Fig. 20 shows the results and it shows that the attack success rate of the adversarial patch under adaptive attacker in Section IV-H2 is consistently close to 0. This indicates the adaptive attacker is not able to successfully generate adversarial patch to evade the mitigation mechanism when 75% of the adversarial pixels are masked. The reason is that a large majority of the adversarial perturbations are removed, and the remainder of perturbations are not able to manipulate the output as intended. This indicates adaptive attack will most likely to be *unsuccessful* in attacking the DNNs with the protection of *Jujutsu*.